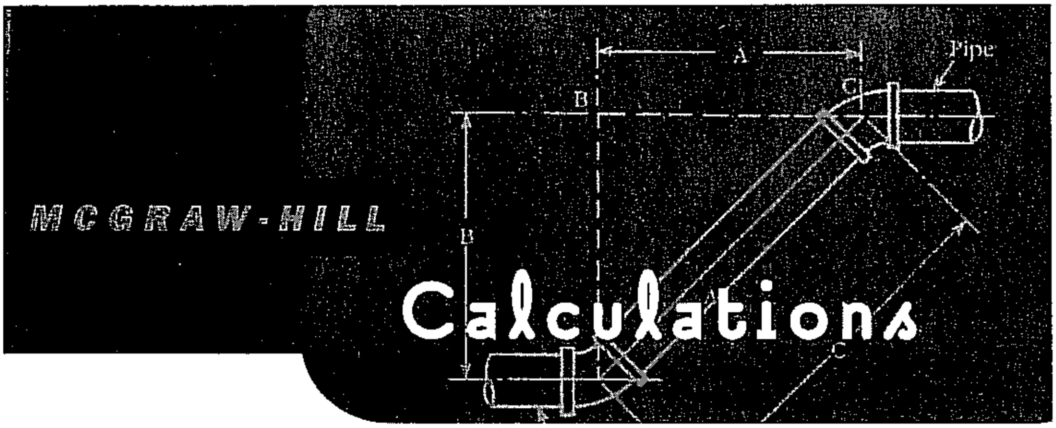

Heat-Transfer Calculations

MYER KUTZ

- Heat-exchanger calculations
- Thermal properties of solid materials
- Conduction heat transfer

Heat-Transfer Calculations

Myer Kutz
Editor

McGraw-Hill
New York Chicago San Francisco Lisbon London Madrid
Mexico City Milan New Delhi San Juan Seoul
Singapore Sydney Toronto

The McGraw-Hill Companies

CIP Data is on file with the Library of Congress

1 2 3 4 5 6 7 8 9 0 DOC/DOC 0 1 0 9 8 7 6 5

ISBN 0-07-141041-4

The sponsoring editor for this book was Kenneth P. McCombs, the editing supervisor was Stephen M. Smith, and the production supervisor was Pamela A. Pelton. It was set in Century Schoolbook by TechBooks. The art director for the cover was Anthony Landi.

Printed and bound by RR Donnelley.

This book is printed on recycled, acid-free paper containing a minimum of 50% recycled, de-inked fiber.

Chapter

23

Calculation of Local Inside-Wall Convective Heat-Transfer Parameters from Measurements of Local Outside-Wall Temperatures along an Electrically Heated Circular Tube

Afshin J. Ghajar and Jae-yong Kim
School of Mechanical and Aerospace Engineering
Oklahoma State University
Stillwater, Oklahoma

Introduction

Heat-transfer measurements in pipe flows are essential for assessment of performance of heat-exchanging equipment and development of heat-transfer correlations. Usually, the experimental procedure for a uniform wall heat flux boundary condition consists of measuring the tube outside-wall temperatures at discrete locations and the inlet and outlet bulk temperatures in addition to other measurements such as the flow rate, voltage drop across the test section, and current carried by the test section. Calculations of the local peripheral heat-transfer coefficients and local Nusselt numbers thereafter are based on knowledge of the tube inside-wall temperatures. Although measurement of the inside-wall temperature is difficult, it can be accurately calculated from the measurements of the outside-wall temperature, the heat generation within the tube, and the thermophysical properties of the pipe material (electrical resistivity and thermal conductivity).

This chapter presents the general finite-difference formulations used for this type of heat-transfer experiment, provides specific applications of the formulations to single- and two-phase convective heat transfer experiments, gives details of implementation of the calculation procedure (finite-difference method) in a computer program, and shows representative reduced heat-transfer results.

Finite-Difference Formulations

The numerical solution of the conduction equation with internal heat generation and non-uniform thermal conductivity and electrical resistivity was originally developed by Farukhi (1973) and introduced by Ghajar and Zurigat (1991) in detail. The numerical solution is based on the following assumptions:

1. Steady-state conditions exist.
2. Peripheral and radial wall conduction exists.
3. Axial conduction is negligible.
4. The electrical resistivity and thermal conductivity of the tube wall are functions of temperature.

On the basis of these assumptions, expressions for calculation of local inside-wall temperature and heat flux and local and average peripheral heat-transfer coefficients will be presented next.

The heat balance on a control volume of the tube at a node P (refer to Fig. 23.1) is given by

$$\dot{q}_g = \dot{q}_n + \dot{q}_e + \dot{q}_s + \dot{q}_w \tag{23.1}$$

From Fourier's law of heat conduction in a given direction n, we have

$$\dot{q} = -kA\frac{dT}{dn} \tag{23.2}$$

Now, substituting Fourier's law and applying the finite-difference formulation for a control volume on a segment (slice) of the tube with nonuniform thermal conductivity in Eq. (23.1), we obtain

$$\dot{q}_n = \left[\frac{\delta_{n^-}}{k_P} + \frac{\delta_{n^+}}{k_N}\right]^{-1} A_n (T_P - T_N) \tag{23.3}$$

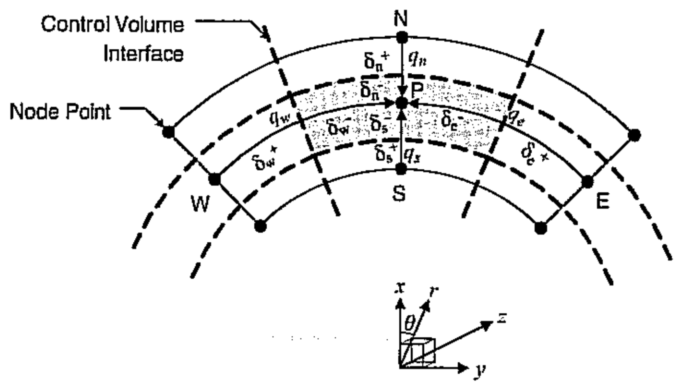

Figure 23.1 Finite-difference node arrangement on a segment (slice).

$$\dot{q}_e = \left[\frac{\delta_{e^-}}{k_P} + \frac{\delta_{e^+}}{k_E}\right]^{-1} A_e\,(T_P - T_E) \tag{23.4}$$

$$\dot{q}_s = \left[\frac{\delta_{s^-}}{k_P} + \frac{\delta_{s^+}}{k_S}\right]^{-1} A_s\,(T_P - T_S) \tag{23.5}$$

$$\dot{q}_w = \left[\frac{\delta_{w^-}}{k_P} + \frac{\delta_{w^+}}{k_W}\right]^{-1} A_w\,(T_P - T_W) \tag{23.6}$$

Note that, in order to deal with the nonuniform thermal conductivity, the thermal conductivity at each control volume interface is evaluated as the sum of the thermal conductivities of the neighboring node points based on the concept that the thermal conductance is the reciprocal of the resistance (Patankar, 1991).

The heat generated at the control volume is given by

$$\dot{q}_g = I^2 R \tag{23.7}$$

Substituting $R = \gamma l / A_c$ into Eq. (23.7) gives

$$\dot{q}_g = I^2 \gamma \frac{l}{A_c} \tag{23.8}$$

Substituting Eqs. (23.3) to (23.6) and (23.8) into Eq. (23.1) and solving for T_S gives

$$T_S = T_P - \left(\dot{q}_g - \dot{q}_n - \dot{q}_e - \dot{q}_w\right) \bigg/ \left\{\left[\frac{\delta_{s^-}}{k_P} + \frac{\delta_{s^+}}{k_S}\right]^{-1} A_s\right\} \tag{23.9}$$

Equation (23.9) is used to calculate the temperature of the interior nodes. Once the local inside-wall temperatures are calculated from Eq. (23.9), the local peripheral inside-wall heat flux can be calculated from the heat-balance equation, Eq. (23.1).

From the local inside-wall temperature, the local peripheral inside-wall heat flux, and the local bulk fluid temperature, the local peripheral heat-transfer coefficient can be calculated as follows:

$$h = \frac{\dot{q}''}{T_w - T_b} \tag{23.10}$$

Note that, in these analyses, it is assumed that the bulk fluid temperature increases linearly from the inlet to the outlet according to the following equation:

$$T_b = T_{\text{in}} + \frac{(T_{\text{out}} - T_{\text{in}})z}{L} \tag{23.11}$$

The local average heat-transfer coefficient at each segment can be calculated by the following equation:

$$\bar{h} = \frac{\dot{q}''}{\bar{T}_w - T_b} \tag{23.12}$$

In this section, we have presented the basic formulations of the local inside-wall temperature, the local peripheral heat-transfer coefficient, the local average heat-transfer coefficient, and the overall heat-transfer coefficient from the given local outside-wall temperature at a particular segment (slice) of an electrically heated circular tube. Next, we will show specific applications of the formulations to single- and two-phase convective heat-transfer experiments.

Application of the Finite-Difference Formulations

In this section, the finite-difference formulations developed in the previous section are applied to actual heat-transfer experiments. The experiments were performed to study single- and two-phase heat transfer in an electrically heated tube under a variety of flow conditions. The obtained data were then used to develop robust single- and two-phase heat-transfer correlations. For this purpose, accurate heat-transfer measurement is critical; therefore, finite-difference formulations were used as a key tool in obtaining accurate heat-transfer coefficients from the measured outside-wall temperatures.

Experimental setup

A brief description of the experimental setup is presented to help the readers understand how the finite-difference formulations are used in actual experimental work.

A schematic diagram of the overall experimental setup is shown in Fig. 23.2. The experimental setup shown in the figure is designed to systemically collect pressure drop and heat-transfer data for single- and two-phase flows for various flow conditions and flow patterns (in case of two-phase flow) and different inclination angles.

The test section is a 27.9-mm i.d. (inside diameter) straight standard stainless-steel 316 schedule 10S pipe with a length : diameter ratio of 100. The uniform wall heat flux boundary condition is maintained by a welder which is a power supply to the test section. The entire length of the test section is insulated using fiberglass pipe wrap insulation, which provides the adiabatic boundary condition for the outside wall. T-type thermocouples are cemented with an epoxy adhesive having high thermal conductivity and electrical resistivity to the outside wall of the test section at uniform intervals of 254 mm (refer to Fig. 23.3). There are 10 thermocouple stations with four thermocouples in 90° peripheral intervals at each station in the test section. The inlet and exit bulk temperatures are measured by T-type thermocouple probes. To ensure a uniform fluid bulk temperature at the inlet and exit of the test section, a mixing well is utilized. More details of the experimental setup may be found in Ghajar et al. (2004).

Heat-transfer measurements at uniform wall heat flux boundary condition are carried out by measuring the outside wall temperatures at the 10 thermocouple stations along the test section and the inlet and outlet bulk temperatures in addition to other measurements such as the flow rates of test fluids, system pressure, voltage drop across the test section, and current carried by the test section.

A National Instruments data acquisition system is used to acquire the data measured during the experiments. The computer interface used to monitor and record the data is a LabVIEW Virtual Instrument written for this specific application.

Finite-difference formulations for the experimental setup

In order to apply the finite-difference formulations developed in the previous section to the experimental setup, the grid configuration of the test section is designed as shown in Fig. 23.4 according to the basic node configuration shown in Fig. 23.1. The computation domain is divided into control volumes of uniform thickness except at the inside

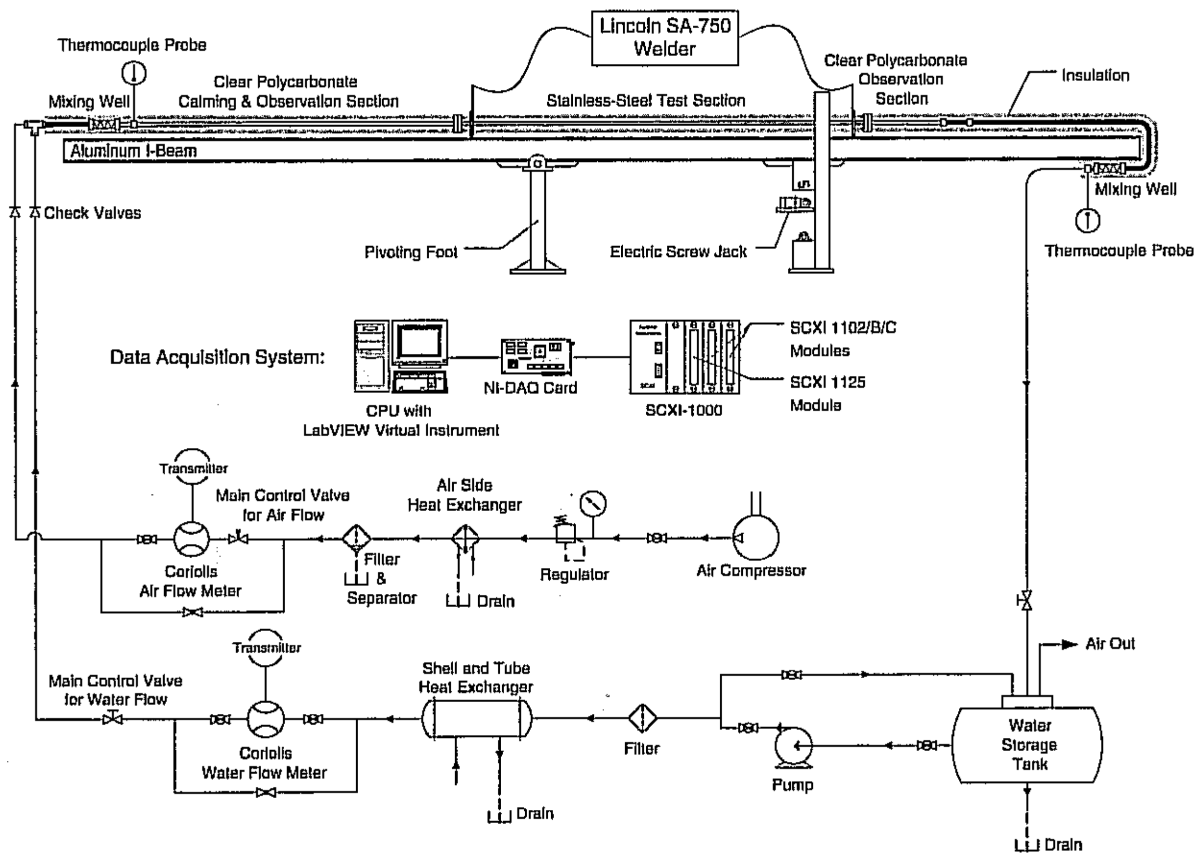

Figure 23.2 Schematic of the experimental setup.

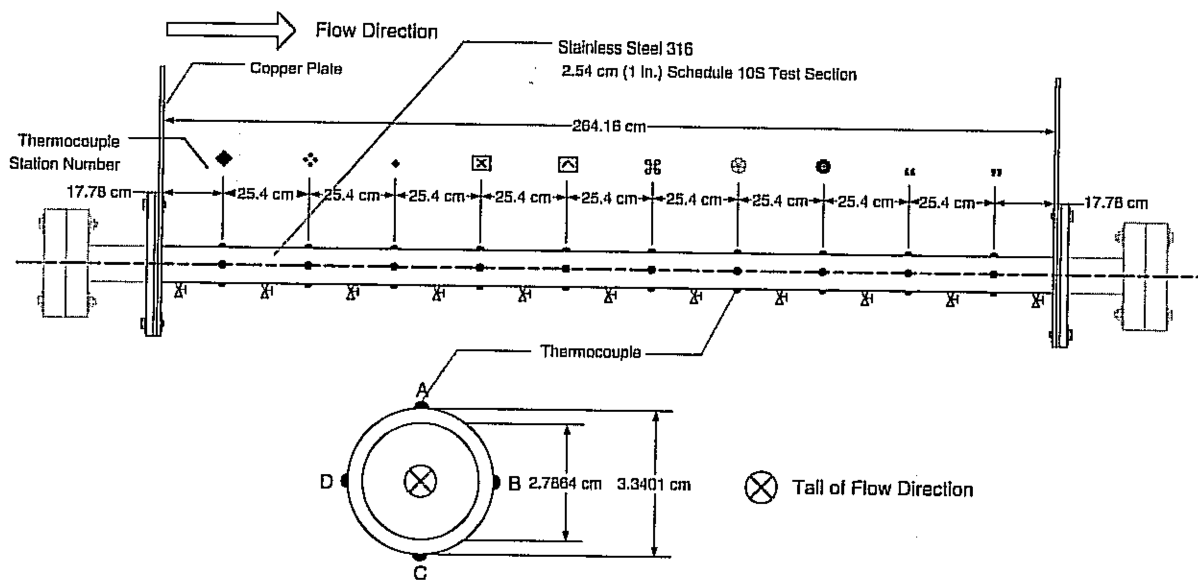

Figure 23.3 Test section.

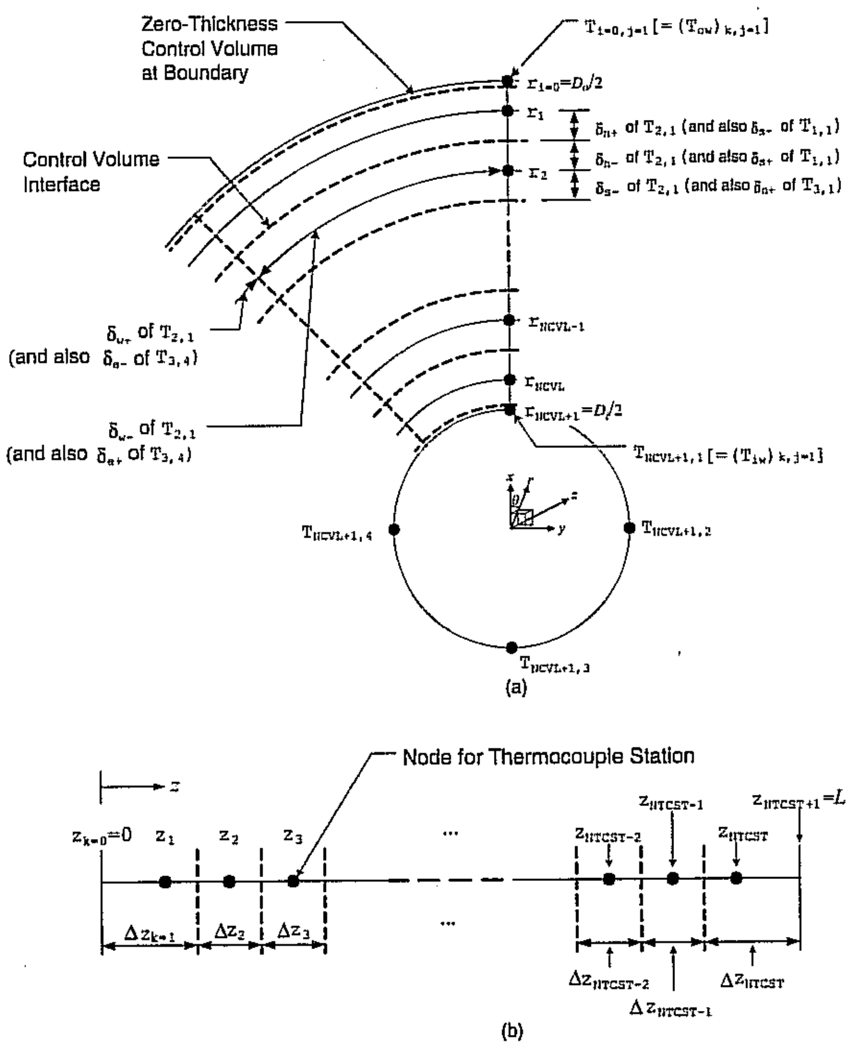

Figure 23.4 Grid configuration for the experimental setup: (*a*) at a segment (slice); (*b*) at axial direction.

and outside walls of the tube in the radial direction, where the control volumes have a zero thickness. The node points are placed in the centerpoint of the corresponding control volumes, and the node points along the circumferential and axial directions are placed in accordance with the actual thermocouple locations at the test section.

According to the assumption that the axial conduction is negligible, each thermocouple station (segment) is solved independently of the others. The calculation in a segment is marched from the outside-wall node points, the temperatures of these nodes are experimentally measured, to the inside-wall node points based on the heat balance at each control volume.

First, determination of the geometric variables at a node point (i, j) is as follows. The distances from a grid point to the interface of the control volume are

$$\delta_{n^+} = \delta_{n^-} = \delta_{s^+} = \delta_{s^-} = \frac{\Delta r}{2} = \frac{(D_o - D_i)/N_{\text{CVL}}}{2} \tag{23.13}$$

for the radial direction and

$$(\delta_{e^+})_i = (\delta_{e^-})_i = (\delta_{w^+})_i = (\delta_{w^-})_i = \frac{2\pi r_i / N_{\text{TC@ST}}}{2} \tag{23.14}$$

for the circumferential direction.

Because of the zero-thickness control volume layer at the boundaries ($i = 0$ and $N_{\text{CVL}} + 1$), we have $\delta_{n^+} = 0$ at $i = 1$ and $\delta_{s^+} = 0$ at $i = N_{\text{CVL}}$.

The areas of all faces for a control volume are

$$(A_n)_i = \frac{2\pi \left[r_i + (\delta_{n^-})_i\right] \Delta z_k}{N_{\text{TC@ST}}} \tag{23.15}$$

$$(A_e)_i = (A_w)_i = \left[(\delta_{n^-})_i + (\delta_{s^-})_i\right] \Delta z_k \tag{23.16}$$

$$(A_s)_i = \frac{2\pi \left[r_i - (\delta_{s^-})_i\right] \Delta z_k}{N_{\text{TC@ST}}} \tag{23.17}$$

The length and the cross-sectional area of the control volume in the axial direction are set as

$$l = \Delta z_k \tag{23.18}$$

$$(A_c)_i = \frac{2\pi r_i \Delta r}{N_{\text{TC@ST}}} \tag{23.19}$$

Now we can calculate the heat generation and the heat flux at a control volume by applying these geometric variables.

Note that because of the zero-thickness control volume layer at the boundaries ($i = 0$ and $N_{\text{CVL}} + 1$), all heat fluxes (q_n, q_e, q_s, and q_w) and the heat generation (q_g) terms are set to zero at $i = 0$ and $N_{\text{CVL}} + 1$.

Therefore, Eqs. (23.3), (23.4), (23.5), (23.6), and (23.8) for $i = 1, 2, \ldots, N_{\text{CVL}}$ and $j = 1, 2, \ldots, N_{\text{TC@ST}}$ become as follows:

$$(\dot{q}_n)_{i,j} = \begin{cases} \dfrac{k_{i,j}}{\delta_{n^-}} (A_n)_i \left(T_{i,j} - T_{i-1,j}\right) & \text{for} \quad i = 1 \\ \left[\dfrac{\delta_{n^-}}{k_{i,j}} + \dfrac{\delta_{n^+}}{k_{i-1,j}}\right]^{-1} (A_n)_i \left(T_{i,j} - T_{i-1,j}\right) & \text{for} \quad i = 2, 3, \ldots, N_{\text{CVL}} \end{cases} \tag{23.20}$$

$$(\dot{q}_e)_{i,j} = \left[\frac{(\delta_{e^-})_i}{k_{i,j}} + \frac{(\delta_{e^+})_i}{k_{i,j+1}}\right]^{-1} (A_e)_i \left(T_{i,j} - T_{i,j+1}\right) \quad \text{for} \quad i = 1, 2, \ldots, N_{\mathrm{CVL}} \tag{23.21}$$

$$(\dot{q}_s)_{i,j} = \begin{cases} \left[\dfrac{\delta_{s^-}}{k_{i,j}} + \dfrac{\delta_{s^+}}{k_{i+1,j}}\right]^{-1} (A_s)_i \left(T_{i,j} - T_{i+1,j}\right) & \text{for} \quad i = 1, 2, \ldots, N_{\mathrm{CVL}} - 1 \\ \dfrac{k_{i,j}}{\delta_{s^-}} (A_s)_i \left(T_{i,j} - T_{i+1,j}\right) & \text{for} \quad i = N_{\mathrm{CVL}} \end{cases} \tag{23.22}$$

$$(\dot{q}_w)_{i,j} = \left[\frac{(\delta_{w^-})_i}{k_{i,j}} + \frac{(\delta_{w^+})_i}{k_{i,j-1}}\right]^{-1} (A_w)_i \left(T_{i,j} - T_{i,j-1}\right) \quad \text{for} \quad i = 1, 2, \ldots, N_{\mathrm{CVL}} \tag{23.23}$$

The heat generated at the control volume is given by

$$\left(\dot{q}_g\right)_{i,j} = I_{i,j}^2 \, \gamma_{i,j} \, \frac{\Delta z_k}{(A_C)_i} \qquad \text{for} \qquad i = 1,\ 2, \ldots,\ N_{\mathrm{CVL}};\ j = 1, 2, \ldots, N_{\mathrm{TC@ST}} \tag{23.24}$$

Substituting Eqs. (23.20) to (23.23) into Eq. (23.1) and solving for $T_{i+1,j}$ gives

$$T_{i+1,j} = \frac{T_{i,j} - \left\{(\dot{q}_g)_{i,j} - (\dot{q}_n)_{i,j} - (\dot{q}_e)_{i,j} - (\dot{q}_w)_{i,j}\right\}}{\left[\dfrac{\delta_{s^-}}{k_{i,j}} + \dfrac{\delta_{s^+}}{k_{i+1,j}}\right]^{-1} (A_s)_i} \tag{23.25}$$

$$\text{for} \qquad i = 0,\ 1,\ 2, \ldots, N_{\mathrm{CVL}};\ j = 1, 2, \ldots, N_{\mathrm{TC@ST}}$$

With $T_{i\,=\,0,j}$ $[= (T_{\mathrm{ow}})_{k,j}]$ given, Eq. (23.25) for the kth thermocouple station will be forced to converge after some iterations since the equation is developed on the basis of heat balance in a control volume.

Then, the local inside-wall temperature at the kth thermocouple station is

$$(T_{\mathrm{iw}})_{k,j} = T_{N_{\mathrm{CVL}}+1,j} \qquad \text{for} \qquad j = 1, 2, \ldots, N_{\mathrm{TC@ST}} \tag{23.26}$$

The local inside-wall heat flux at the kth thermocouple station is

$$\left(\dot{q}''_{\mathrm{in}}\right)_{k,j} = k_{N_{\mathrm{CVL}},j} \frac{T_{N_{\mathrm{CVL}},j} - T_{N_{\mathrm{CVL}}+1,j}}{\Delta r/2} \qquad \text{for} \qquad j = 1, 2, \ldots, N_{\mathrm{TC@ST}} \tag{23.27}$$

The bulk temperature at the kth thermocouple station is

$$(T_b)_k = T_{\text{in}} + \frac{(T_{\text{out}} - T_{\text{in}})z_k}{L} \tag{23.28}$$

The local heat-transfer coefficient at the kth thermocouple station is

$$h_{k,j} = \frac{\left(\dot{q}''_{\text{in}}\right)_{k,j}}{(T_{\text{iw}})_{k,j} - (T_b)_k} \qquad \text{for} \qquad j = 1, 2, \ldots, N_{\text{TC@ST}} \tag{23.29}$$

Finally, the local average heat-transfer coefficient at the kth thermocouple station is

$$\bar{h}_k = \frac{\dfrac{1}{N_{\text{TC@ST}}} \displaystyle\sum_{j=1}^{N_{\text{TC@ST}}} \left(\dot{q}''_{\text{in}}\right)_{k,j}}{\dfrac{1}{N_{\text{TC@ST}}} \displaystyle\sum_{j=1}^{N_{\text{TC@ST}}} (T_{\text{iw}})_{k,j} - (T_b)_k} \tag{23.30}$$

At times it is necessary to calculate the overall heat-transfer coefficient for certain test runs. In these cases, the overall heat-transfer coefficient can be calculated as follows:

$$\bar{h} = \frac{1}{L} \int \bar{h}\, dz = \frac{1}{L} \sum_{k=1}^{N_{\text{TCST}}} \bar{h}_k \, \Delta z_k \tag{23.31}$$

Note that, to execute these calculations, the thermophysical properties of the pipe material (thermal conductivity and electrical resistivity) are required. These and other thermophysical properties needed for these type of calculations will be presented next.

Thermophysical properties

In order to implement the formulations above in a computer program and represent the heat transfer and flow data in a dimensionless form, knowledge of thermophysical properties of pipe material and the working fluids are required. For the heat-transfer experiments presented in this chapter to demonstrate the applications of the finite-difference formulations, the pipe material was made of stainless steel 316 and the working fluids were air, water, ethylene glycol, and mixtures of ethylene glycol and water. The equations used in Tables 23.1 to 23.4 present the necessary equations for the calculation of the pertinent thermophysical properties. The equations presented were mostly curve fitted from the available data in the literature for the range of experimental temperatures.

TABLE 23.1 Equations for Thermophysical Properties of Stainless Steel 316

Fitted equation	Range and accuracy	Data source
Thermal conductivity: $k_{ss} = 13.0 + 1.6966 \times 10^{-2}\,T - 2.1768 \times 10^{-6}T^2$, with T in °C and k_{ss} in W/m-K	300–1000 K; $R^2 = 0.99985$	Incropera and Dewitt (2002)
Electrical resistivity: $\gamma_{ss} = 73.152 + 6.7682 \times 10^{-2}T - 2.6091 \times 10^{-6}T^2 - 2.2713 \times 10^{-8}T^3$, with T in °C and γ_{ss} in μΩ-cm	−196 to 600°C; $R^2 = 0.99955$	Davis (1994)

TABLE 23.2 Equations for Thermophysical Properties of Air

Fitted equation	Range and accuracy	Data source
Density: $\rho_{air} = p/[T(R/M_{air})]$, where T is in kelvins, ρ_{air} in kg/m^3, p is absolute pressure in Pa, R is the universal gas constant (= 8314.34 J/kmol · K), and M_{air} is the molecular weight of air (= 28.966 kg/kmol)		
Viscosity: $\mu_{air} = 1.7211 \times 10^{-5} + 4.8837 \times 10^{-8}T - 2.9967 \times 10^{-11}T^2$, with T in °C and μ_{air} in Pa · s	−10 to 120°C; $R^2 = 0.99994$	Kays and Crawford (1993)
Thermal conductivity: $k_{air} = 2.4095 \times 10^{-2} + 7.6997 \times 10^{-5}T - 5.189 \times 10^{-8}T^2$, with T in °C and k_{air} in W/m · K	−10 to 120°C; $R^2 = 0.99996$	Kays and Crawford (1993)
Specific heat: $(c_p)_{air} = 1003.6 + 3.1088^{-2}T + 3.4967 \times 10x^{-4}T^2$, with T in °C and $(c_p)_{air}$ in J/kg · K	−10 to 330°C; $R^2 = 0.99956$	Kays and Crawford (1993)

TABLE 23.3 Equations for Thermophysical Properties of Water

Fitted equation	Range and accuracy	Data source
Density: $\rho_{water} = 999.96 + 1.7158 \times 10^{-2}T - 5.8699 \times 10^{-3}T^2 + 1.5487 \times 10^{-5}T^3$, with T in °C and ρ_{water} in kg/m^3	0–100°C; $R^2 = 0.99997$	Linstrom and Mallard (2003)
Viscosity: $\mu_{water} = 1.7888 \times 10^{-3} - 5.9458 \times 10^{-5}T + 1.3096 \times 10^{-6}T^2 - 1.8035 \times 10^{-8}T^3 + 1.3446 \times 10^{-10}T^4 - 4.0698 \times 10^{-13}T^5$, with T in °C and μ_{water} in Pa · s	0–100°C; $R^2 = 0.99998$	Linstrom and Mallard (2003)
Thermal conductivity: $k_{water} = 5.6026 \times 10^{-1} - 2.1056 \times 10^{-3}T - 8.6806 \times 10^{-6}T^2 - 5.4451 \times 10^{-9}T^3$, with T in °C and k_{water} in W/m · K	0–100°C; $R^2 = 0.99991$	Linstrom and Mallard (2003)
Specific heat: $(c_p)_{water} = 4219.8728 - 3.3863T + 0.11411T^2 - 2.1013 \times 10^{-3}T^3 + 2.3529 \times 10^{-5}T^4 - 1.4167 \times 10^{-7}T^5 + 3.58520 \times 10^{-10}T^6$, with T in °C and $(c_p)_{water}$ in J/kg · K	0–100°C; $R^2 = 0.99992$	Linstrom and Mallard (2003)

TABLE 23.4 Equations for Thermophysical Properties of Mixture of Ethylene Glycol and Water

Fitted equation	Range and accuracy	Data source
Density:		
$\rho_{mix} = \sum_{i=1}^{3} \sum_{j=1}^{3} C_{ij} X^{(j-1)} T^{(i-1)}$ where $C = \begin{pmatrix} 1.0004 & 0.17659 & -0.049214 \\ -1.2379 \times 10^{-4} & -9.9189 \times 10^{-4} & 4.1024 \times 10^{-4} \\ -2.9837 \times 10^{-6} & 2.4264 \times 10^{-6} & -9.5278 \times 10^{-8} \end{pmatrix}$ with T in °C and ρ_{mix} in g/cm^3	0–150°C within ±0.25%	Ghajar and Zurigat (1991)
Viscosity:		
$\ln \mu_{mix} = \sum_{i=1}^{2} \sum_{j=1}^{3} C_{ij} X^{(j-1)} T^{(i-1)} + \left[\sum_{j=1}^{3} C_{3j} X^{(j-1)} \right]^{1/4} T^2$ where $C = \begin{pmatrix} 0.55164 & 2.6492 & 0.82935 \\ -2.7633 \times 10^{-2} & -3.1496 \times 10^{-2} & 4.8136 \times 10^{-3} \\ -6.0629 \times 10^{-17} & 2.2389 \times 10^{-15} & -5.8790 \times 10^{-16} \end{pmatrix}$ with T in °C and μ_{mix} in mPa · s	−10 to 100°C within ±5%	Ghajar and Zurigat (1991)

TABLE 23.4 Equations for Thermophysical Properties of Mixture of Ethylene Glycol and Water (*Continued*)

Fitted equation	Range and accuracy	Data source
Prandtl number: $\ln \mathrm{Pr}_{\mathrm{mix}} = \sum_{i=1}^{2}\sum_{j=1}^{3} C_{ij} X^{(j-1)} T^{(i-1)} + \left[\sum_{j=1}^{3} C_{3j} X^{(j-1)}\right]^{1/4} T^2$ where $C = \begin{pmatrix} 2.5735 & 3.0411 & 0.60237 \\ -3.1169 \times 10^{2} & -2.5424 \times 10^{-2} & 3.7454 \times 10^{-3} \\ 1.1605 \times 10^{-16} & 2.5283 \times 10^{-15} & 2.3777 \times 10^{-17} \end{pmatrix}$ with T in °C	−10 to 100°C within ±5%	Ghajar and Zurigat (1991)
Thermal conductivity: $k_{\mathrm{mix}} = (1 - X)\,k_{\mathrm{water}} + X k_{\mathrm{eg}} - k_F\,(k_{\mathrm{water}} - k_{\mathrm{eg}})\,(1 - X)\,X$ where $k_{\mathrm{eg}} = 0.24511 + 1.755 \times 10^{-4} T - 8.52 \times 10^{-7} T^2$, $k_F = 0.6635 - 0.3698X - 8.85 \times 10^{-4} T$, with T in °C and k_{water}, k_{eg}, k_F, and k_{mix} in W/m · K	0–150°C within ±1%	Ghajar and Zurigat (1991)
Thermal expansion coefficient: $\beta_{\mathrm{mix}} = -\frac{1}{\rho_{\mathrm{mix}}} \left\{ \begin{array}{l} -1.2379 \times 10^{-4} - 9.9189 \times 10^{-4} X + 4.1024 \times 10^{-4} X^2 \\ +2\left(-2.9837 \times 10^{-6} + 2.4614 \times 10^{-6} X - 9.5278 \times 10^{-8} X^2\right) T \end{array} \right\}$ with T in °C, ρ_{mix} in g/cm^3, and β_{mix} in 1/°C	0–150°C within ±0.25%	Ghajar and Zurigat (1991)

Stainless steel 316. In the finite-difference equations, the thermal conductivity and electrical resistivity of each node are determined as a function of temperature from the equations shown in Table 23.1 for stainless steel 316.

Test fluids. The test fluids used in the experiments were air, distilled water, ethylene glycol, and different mixtures of distilled water and ethylene glycol. The equations for thermophysical properties of these fluids are presented in Tables 23.2 to 23.4.

Computer program

The finite-difference formulations presented in the previous section are implemented into a computer program written for the experimental works described in this chapter. The computer program consists of five parts: reading and reducing input data, executing the finite-difference formulations, providing thermophysical properties, evaluating all the heat-transfer and flow parameters, and printing outputs. Since the finite-difference formulations and thermophysical properties have already been discussed in detail, the inputs and outputs from the computer program will be presented next.

Input data. All the necessary inputs for the computer program are provided by a database file managing a data set and each raw data file for the data set. The raw data file is produced through recordings from the experimental data acquisition process. A sample of the input files is given as Fig. 23.5*a* and *b*.

The database file shown in Fig. 23.5*a* includes the preset information for an experimental run:

`GroupNo`	Data group number (e.g., the first digit indicates 1→single-phase, 2→two-phase)
`RunNo`	Test run number
`Phase`	1→single-phase flow test, 2→two-phase flow test
`Liquid`	Test liquid (W→water, G→ethylene glycol)
`MC_EG`	Mass fraction of ethylene glycol in the liquid mixture
`Pattern`	Flow pattern information of the two-phase flow test
`IncDeg`	Inclination angle of the test section

With the information provided in the database file, the computer program opens and reads data from each individual raw data file for an experimental run shown in Fig. 23.5*b* and proceeds to all the required data reductions and calculations and then saves the results in an output file for each test run.

Output. A sample of the outputs from the computer program is shown in Figs. 23.6 and 23.7 for a single-phase flow experimental run and a

GroupNo	RunNo	Phase	Liquid	MC_EG	Pattern	IncDeg
1010	RN0608	1	W	0.00	NONE	0.00
1020	RN0709	1	G	0.50	NONE	0.00
2010	RN4438	2	W	0.00	A	0.00
2210	RN4658	2	W	0.00	ABS	2.00
2510	RN8750	2	W	0.00	BS	5.00
2710	RN4860	2	W	0.00	S	7.00
...						

(a)

Date	Time	TC01-1	TC01-2	TC01-3	TC01-4	...	TP_IN	TP_OUT	...	FR_w	FR_a	Ref.P	Current	Voltage
MM-DD-YYYY	HH:MM:SS	C	C	C	C	...	C	C	...	lb/min	lb/min	psi	A	V
11-29-2003	06:47:14	24.876	21.110	16.341	21.391	...	15.988	21.039	...	2.659	1.662	2.459	299.746	2.299
11-29-2003	06:47:23	24.861	21.069	16.341	21.399	...	15.988	21.038	...	2.770	1.658	2.437	299.732	2.299
11-29-2003	06:47:31	24.860	21.045	16.347	21.353	...	15.994	21.048	...	2.656	1.669	2.460	299.746	2.300
11-29-2003	06:47:40	24.864	21.021	16.343	21.367	...	15.986	21.049	...	2.659	1.668	2.430	299.553	2.299
11-29-2003	06:47:49	24.862	20.978	16.342	21.316	...	15.988	21.055	...	2.657	1.659	2.439	299.679	2.299
11-29-2003	06:47:57	24.852	21.008	16.342	21.320	...	15.991	21.063	...	2.658	1.663	2.472	299.865	2.300
11-29-2003	06:48:06	24.856	21.086	16.343	21.331	...	16.007	21.050	...	2.663	1.667	2.457	299.877	2.300
...														

(b)

Figure 23.5 Input data formats. (*a*) Database format for experimental run; (*b*) raw data format for experimental run.

```
=================================================
               RUN NUMBER 0608
              SINGLE PHASE TEST
             TEST FLUID IS WATER
            Test Date: 04-01-2003
              FPS UNIT VERSION
=================================================

MASS FLOW RATE          =    1308.3   LBM/HR
MASS FLUX               =    199333   LBM/(SQ.FT-HR)
FLUID VELOCITY          =       .88   FT/S
ROOM TEMPERATURE        =     73.32   F
INLET TEMPERATURE       =     80.74   F
OUTLET TEMPERATURE      =     87.07   F
AVERAGE RE NUMBER       =      9213
AVERAGE PR NUMBER       =      5.59
CURRENT TO TUBE         =     535.0   AMPS
VOLTAGE DROP IN TUBE    =      4.29   VOLTS
AVERAGE HEAT FLUX       =      3161   BTU/(SQ.FT-HR)
Q=AMP*VOLT              =      7831   BTU/HR
Q=M*C*(T2-T1)           =      8267   BTU/HR
HEAT BALANCE ERROR      =     -5.57   %
```

(a)

OUTSIDE SURFACE TEMPERATURES [F]

	1	2	3	4	5	6	7	8	9	10
1	93.99	95.63	96.36	97.01	97.01	97.88	98.40	98.97	99.78	100.26
2	94.21	96.01	96.72	96.94	97.56	98.30	98.89	99.53	100.20	100.90
3	93.67	95.70	96.86	97.19	97.87	98.23	99.10	99.25	100.59	101.33
4	93.24	95.59	96.49	97.23	97.37	98.22	98.53	99.30	100.04	100.34

INSIDE SURFACE TEMPERATURES [F]

	1	2	3	4	5	6	7	8	9	10
1	92.31	93.94	94.67	95.32	95.31	96.18	96.71	97.27	98.08	98.56
2	92.53	94.33	95.03	95.25	95.87	96.61	97.20	97.85	98.51	99.21
3	91.98	94.01	95.18	95.50	96.19	96.54	97.42	97.56	98.91	99.65
4	91.54	93.90	94.80	95.54	95.68	96.53	96.84	97.61	98.35	98.64

REYNOLDS NUMBER AT THE INSIDE TUBE WALL

	1	2	3	4	5	6	7	8	9	10
1	10161	10349	10434	10509	10509	10610	10671	10738	10833	10889
2	10186	10394	10476	10501	10574	10660	10729	10805	10883	10966
3	10123	10357	10493	10531	10610	10652	10754	10771	10930	11018
4	10073	10345	10449	10535	10551	10651	10687	10778	10864	10899

INSIDE SURFACE HEAT FLUXES [BTU/HR/FT^2]

	1	2	3	4	5	6	7	8	9	10
1	2923	2938	2942	2939	2950	2949	2949	2953	2953	2954
2	2920	2925	2933	2941	2934	2933	2936	2931	2943	2942
3	2932	2937	2929	2934	2927	2940	2930	2946	2931	2926
4	2946	2936	2939	2933	2940	2935	2946	2937	2947	2957

PERIPHERAL HEAT TRANSFER COEFFICIENT BTU/(SQ.FT-HR-F)

	1	2	3	4	5	6	7	8	9	10
1	262	241	239	238	251	246	248	249	245	247
2	257	233	231	240	239	236	237	235	235	234
3	271	240	229	234	232	238	232	242	227	224
4	283	242	236	233	243	238	245	241	239	246

(b)

Figure 23.6 Output for single-phase flow heat-transfer test run. (*a*) Part 1: summary of a test run. (*b*) Part 2: detailed information at each thermocouple location. (*c*) Part 3: detailed information at each thermocouple station.

RUN NUMBER 0608 CONTINUED
SINGLE PHASE TEST
TEST FLUID IS WATER
Test Date: 04-01-2003
FPS UNIT VERSION

ST	RE	PR	X/D	MUB	MUW	TB	TW	DENS	NU
1	8911.67	5.80	6.38	2.045	1.798	81.17	92.09	62.20	69.71
2	8978.30	5.75	15.50	2.030	1.759	81.77	94.04	62.20	62.10
3	9045.13	5.71	24.61	2.015	1.742	82.38	94.92	62.19	60.77
4	9112.15	5.66	33.73	2.000	1.732	82.99	95.40	62.18	61.35
5	9179.36	5.61	42.84	1.985	1.725	83.60	95.76	62.18	62.56
6	9246.76	5.57	52.96	1.971	1.712	84.21	96.47	62.17	62.05
7	9314.36	5.52	61.08	1.956	1.701	84.82	97.04	62.17	62.21
8	9382.14	5.48	70.19	1.942	1.691	85.43	97.57	62.16	62.58
9	9450.11	5.43	79.31	1.928	1.675	86.04	98.46	62.15	61.15
10	9518.27	5.39	88.42	1.914	1.665	86.64	99.02	62.15	61.39

NOTE: TBULK IS GIVEN IN DEGREES FAHRENHEIT
MUB AND MUW ARE GIVEN IN LBM/(FT*HR)

(c)

Figure 23.6 *(Continued)*

two-phase flow experimental run, respectively. As shown in the figures [Fig. 23.6 is in English units and Fig. 23.7 is in SI (metric) units], the user has the option of specifying SI or English units for the output.

The output file starts with a summary of some of the important information about the experimental run for a quick reference as shown in Figs. 23.6*a* and 23.7*a*. The program then lists (see Figs. 23.6*b* and 23.7*b*) the measured outside-wall temperatures, the calculated inside-wall temperatures, the calculated Reynolds numbers (superficial Reynolds numbers for each phase of the two-phase flow run) of the flow based on the inside-wall temperature, the calculated heat flux, and the calculated peripheral heat-transfer coefficients for each thermocouple location. In the last part of the output (refer to Figs. 23.6*c* and 23.7*c*), the tabulated summary of the local averaged heat-transfer results at each thermocouple station, such as its location from the tube entrance, bulk Reynolds numbers, bulk Prandtl numbers, viscosities at the wall and bulk, local average heat-transfer coefficient, and Nusselt numbers are displayed. In the case of two-phase flow runs, some auxiliary information for the two-phase flow parameters is listed as shown in Fig. 23.7*d*. More details about the information that appears in Fig. 23.7*d* may be found in Ghajar (2004).

Utilization of the finite-difference formulations

The outputs presented in Figs. 23.6 and 23.7 contain all the necessary information for an in-depth analysis of the experiments. One way

```
===============================================
                RUN NUMBER 4897
                TWO-PHASE TEST
              FLOW PATTERN: ABS
            Test Date: 04-01-2004
               SI UNIT VERSION
===============================================
LIQUID                        :     WATER
GAS                           :       AIR
LIQUID MASS FLOW RATE         :   1370.36 [kg/hr]
GAS    MASS FLOW RATE         :    33.902 [kg/hr]
LIQUID V_SL                   :     0.625 [m/s]
GAS    V_SG                   :     6.482 [m/s]
ROOM   TEMPERATURE            :     14.89 [C]
INLET  TEMPERATURE            :     13.67 [C]
OUTLET TEMPERATURE            :     14.70 [C]
AVG REFERENCE GAGE PRESSURE   :  95165.30 [Pa]
AVG LIQUID RE_SL              :     14962
AVG GAS    RE_SG              :     24043
AVG LIQUID PR_L               :     8.278
AVG GAS    PR_G               :     0.714
AVG LIQUID DENSITY            :     999.1 [kg/m^3]
AVG GAS    DENSITY            :     2.382 [kg/m^3]
AVG LIQUID SPECIFIC HEAT      :     4.190 [kJ/kg-K]
AVG GAS    SPECIFIC HEAT      :     1.004 [kJ/kg-K]
AVG LIQUID VISCOSITY          : 116.25e-05 [Pa-s]
AVG GAS    VISCOSITY          : 17.90e-06 [Pa-s]
AVG LIQUID CONDUCTIVITY       :     0.588 [W/m-K]
AVG GAS    CONDUCTIVITY       : 25.18e-03 [W/m-K]
CURRENT TO TUBE               :    466.13 [A]
VOLTAGE DROP IN TUBE          :      3.54 [V]
AVG HEAT FLUX                 :   7138.39 [W/m^2]
Q = AMP*VOLT                  :   1650.66 [W]
QGEN CALCULATED               :   1600.13 [W]
QGEN CALCULATION ERROR        :     -3.06 [%]
Q = M*C*(T2 -T1)              :   1652.02 [W]
HEAT BALANCE ERROR            :      0.08 [%]
```

(a)

OUTSIDE SURFACE TEMPERATURE OF TUBE [C]

	1	2	3	4	5	6	7	8	9	10
1	16.71	17.09	17.35	17.64	17.83	18.11	18.11	18.31	18.12	18.25
2	16.17	16.28	16.65	16.69	16.97	17.14	17.26	17.03	17.33	17.33
3	15.55	15.71	15.75	15.89	16.18	16.20	16.35	16.23	16.33	16.40
4	16.23	16.38	16.41	16.70	16.85	17.01	17.18	17.26	17.13	17.30

INSIDE SURFACE TEMPERATURES [C]

	1	2	3	4	5	6	7	8	9	10
1	16.02	16.41	16.66	16.95	17.15	17.43	17.43	17.63	17.43	17.57
2	15.48	15.58	15.95	16.00	16.27	16.44	16.56	16.33	16.63	16.64
3	14.84	15.00	15.04	15.18	15.47	15.49	15.64	15.52	15.62	15.69
4	15.54	15.68	15.71	16.00	16.15	16.31	16.48	16.57	16.43	16.60

SUPERFICIAL REYNOLDS NUMBER OF GAS AT THE INSIDE TUBE WALL

	1	2	3	4	5	6	7	8	9	10
1	23925	23901	23885	23866	23854	23836	23836	23824	23836	23828
2	23960	23954	23930	23927	23910	23899	23891	23906	23887	23886
3	24001	23991	23988	23979	23961	23959	23950	23957	23951	23947
4	23956	23947	23945	23927	23918	23907	23896	23891	23900	23888

SUPERFICAL REYNOLDS NUMBER OF LIQUID AT THE INSIDE TUBE WALL

	1	2	3	4	5	6	7	8	9	10
1	15718	15878	15965	16107	16188	16309	16307	16391	16310	16366
2	15492	15533	15689	15707	15823	15893	15943	15848	15974	15975
3	15230	15297	15311	15369	15488	15498	15558	15511	15550	15580
4	15517	15577	15589	15710	15770	15837	15911	15945	15887	15961

INSIDE SURFACE HEAT FLUXES [W/m^2]

	1	2	3	4	5	6	7	8	9	10
1	6840	6805	6797	6781	6785	6768	6791	6752	6791	6785
2	6909	6935	6903	6929	6925	6924	6918	6956	6906	6922
3	7011	7007	7032	7038	7028	7049	7050	7057	7055	7058
4	6900	6920	6938	6928	6943	6944	6929	6923	6936	6926

PERIPHERAL HEAT TRANSFER COEFFICIENT [W/m^2-K]

	1	2	3	4	5	6	7	8	9	10
1	3002	2655	2499	2329	2258	2119	2198	2117	2343	2313
2	3988	3998	3436	3545	3245	3144	3111	3667	3291	3458
3	6386	6029	6407	6180	5288	5622	5425	6502	6529	6691
4	3846	3761	3923	3530	3458	3357	3229	3252	3667	3516

(b)

Figure 23.7 Output for two-phase flow heat-transfer experimental run. (*a*) Part 1: summary of a test run. (*b*) Part 2: detailed information at each thermocouple location. (*c*) Part 3: detailed information at each thermocouple station. (*d*) Part 4: auxiliary information.

RUN NUMBER 4897 CONTINUED
TWO-PHASE TEST
FLOW PATTERN: ABS
Test Date: 04-01-2004
SI UNIT VERSION

ST	X/D	RESL	RESG	PRL	PRG	HUB/W(L)	HUB/W(G)	HT/HB	HFLUX	TB[C]	TW[C]	HCOEFF	NU_L
1	6.38	14781	24072	8.39	0.714	1.048	0.995	0.470	6915	13.74	15.47	4006.7	190.01
2	15.50	14821	24065	8.37	0.714	1.051	0.995	0.440	6917	13.84	15.67	3790.2	179.69
3	24.61	14861	24059	8.34	0.714	1.053	0.995	0.390	6918	13.94	15.84	3643.0	172.66
4	33.73	14902	24053	8.32	0.714	1.055	0.995	0.377	6919	14.04	16.03	3473.7	164.58
5	42.84	14942	24046	8.29	0.714	1.059	0.994	0.427	6920	14.14	16.26	3265.9	154.69
6	51.96	14983	24040	8.27	0.714	1.060	0.994	0.377	6921	14.24	16.42	3175.8	150.37
7	61.08	15023	24033	8.24	0.714	1.060	0.994	0.405	6922	14.34	16.53	3161.4	149.65
8	70.19	15064	24027	8.22	0.714	1.057	0.994	0.326	6922	14.44	16.51	3335.6	157.84
9	79.31	15104	24021	8.19	0.714	1.055	0.995	0.359	6922	14.54	16.53	3474.5	164.37
10	88.42	15145	24014	8.17	0.714	1.054	0.995	0.346	6923	14.63	16.62	3478.9	164.52

(c)

RUN NUMBER 4897 CONTINUED
TWO-PHASE TEST
FLOW PATTERN: ABS
Test Date: 04-01-2004
SI UNIT VERSION

INCLINATION ANGLE	:	7.000	[DEG]
TOTAL MASS FLUX(Gt)	:	639.699	[kg/m^2-s]
QUALITY(x)	:	0.024	
SLIP RATIO(K)	:	3.332	
VOID FRACTION(alpha)	:	0.757	
V_SL	:	0.625	[m/s]
V_SG	:	6.482	[m/s]
RE_SL	:	14962	
RE_SG	:	24043	
RE_TP	:	39005	
X(Taitel & Dukler)	:	2.070	
T(Taitel & Dukler)	:	0.139	
Y(Taitel & Dukler)	:	27.098	
F(Taitel & Dukler)	:	0.609	
K(Taitel & Dukler)	:	74.440	

(d)

Figure 23.7 (*Continued*)

to verify the reliability of the finite-difference formulations is to compare the experimental heat-transfer coefficients with the predictions from the well-known empirical heat-transfer correlations. Figure 23.8 shows the comparison of the experimental Nusselt numbers (dimensionless heat-transfer coefficients) obtained from the computer program with those calculated from selected well-known single-phase heat-transfer correlations of Colburn (1933), Sieder and Tate (1936), Gnielinski (1976), and Ghajar and Tam (1994). As shown in the figure, the majority of the experimental data is excellently matched with the calculated values from the correlations, and the maximum deviation between the calculated and the experimental values is within ±20 percent. Note that in Fig. 23.8 Gnielinski's (1976) correlations, labeled as [1] and [3], refer to the first and the third correlations proposed in his work.

The finite-difference formulations presented here have been successfully applied to develop correlation in single- and two-phase flow convective heat-transfer studies. Ghajar and Tam (1994) utilized the

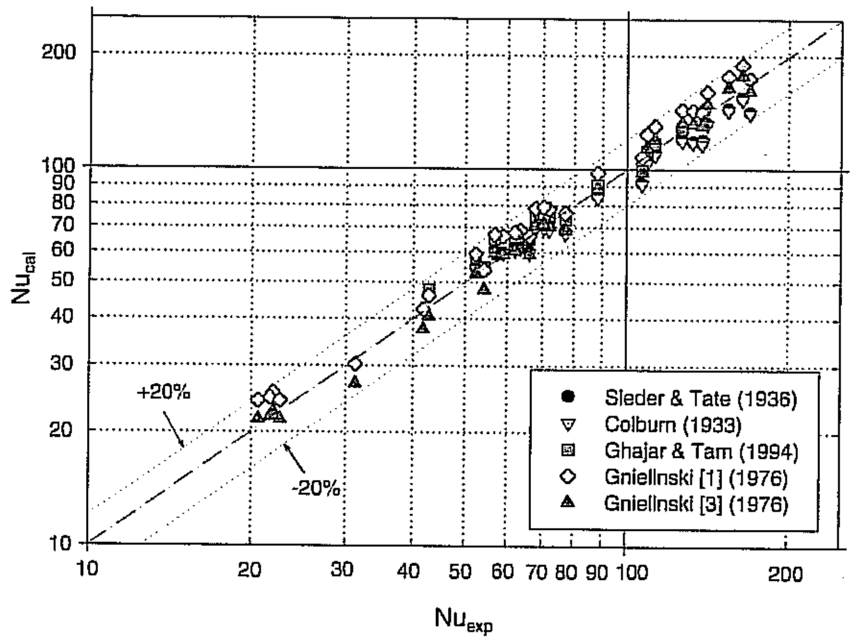

Figure 23.8 Comparison of experimental Nusselt numbers with predictions from selected single-phase heat-transfer correlations at thermocouple station 6.

finite-difference formulations for heat-transfer measurements in a horizontal circular straight tube with three different inlet configurations (reentrant, square-edged, and bell-mouth inlets) under uniform wall heat flux boundary condition. From the measurements, they successfully developed a correlation for prediction of the developing and fully developed forced and mixed single-phase convective heat-transfer coefficients in the transition region for each inlet. They also proposed heat-transfer correlations for laminar, transition, and turbulent regions for the three inlets.

In the case of the gas-liquid two-phase flow heat transfer, Kim and Ghajar (2002) applied the finite-difference formulations in order to measure heat-transfer coefficients and developed correlations for the overall heat-transfer coefficients with different flow patterns in a horizontal tube. A total of 150 two-phase heat-transfer experimental data were used to develop the heat-transfer correlations. Ghajar et al. (2004) extended the work of Kim and Ghajar (2002) and studied the effect of slightly upward inclination (2°, 5°, and 7°) on heat transfer in two-phase flow.

In the research works mentioned here, a computer program based on the presented finite-difference formulations was used as the key tool to analyze the experimental data. As demonstrated, the computational procedure (computer program) presented in this chapter can be utilized as an effective design tool to perform parametric studies or to develop heat-transfer correlations. It can also be used as a demonstration tool for the basic principles of heat conduction and convection.

Summary

A detailed computational procedure has been developed to calculate the local inside-wall temperatures and the local peripheral convective heat-transfer coefficients from the local outside-wall temperatures measured at different axial locations along an electrically heated circular tube (uniform wall heat flux boundary condition). The computational procedure is based on finite-difference formulation and the knowledge of heat generation within the pipe wall and the thermophysical properties of the pipe material and the working fluids. The method has applications in a variety industrial heat-exchanging equipment and can be used to reduce the heat-transfer experimental data to a form suitable for development of forced- and mixed-convection flow heat-transfer correlations in an electrically heated circular tube for different flow regimes.

Nomenclature

A	Area, m^2
A_c	Cross-sectional area of a control volume in the axial direction, m^2
C	Coefficient; refer to Table 23.4
c_p	Specific heat at constant pressure, $J/(kg \cdot K)$
D_i	Circular tube inside diameter, m
D_o	Circular tube outside diameter, m
E	Neighboring node point to a given node point in the eastern direction; refer to Fig. 23.1
h	Heat-transfer coefficient, $W/(m^2 \cdot K)$
$\bar{h}$	Local average heat-transfer coefficient, $W/(m^2 \cdot K)$; refer to Eqs. (23.12) and (23.30)
$\bar{\bar{h}}$	Overall heat-transfer coefficient, $W/(m^2 \cdot K)$; refer to Eq. (23.31)
I	Electrical current, A
i	Index in the radial direction
j	Index in the circumferential direction
k	Thermal conductivity, $W/(m \cdot K)$, or index in the axial direction
L	Length of the test section, m

l	Length of a control volume in the axial direction, m
N	Neighboring node point to a given node point in the northern direction; refer to Fig. 23.1
N_{CVL}	Number of control volume layers in the radial direction except the boundary layers
$N_{TC@ST}$	Number of thermocouples at a thermocouple station
N_{TCST}	Number of thermocouple stations
Nu	Nusselt number, hD_i/k, dimensionless
n	Normal distance, m
P	A given node point P; refer to Fig. 23.1
Pr	Prandtl number, $\mu c_p/k$, dimensionless
p	Pressure, Pa
$\dot{q}$	Heat-transfer rate, W
$\dot{q}_g$	Heat generation rate, W
$\dot{q}''$	Heat flux, W/m^2
R	Electrical resistance, Ω or the universal gas constant (= 8314.34 J/kmol · K)
R^2	Correlation coefficient, dimensionless
r	Radius, m
T	Temperature, °C or K
S	Neighboring node point to a given node point in the southern direction; refer to Fig. 23.1
W	Neighboring node point to a given node point in the western direction; refer to Fig. 23.1
X	Mass fraction of ethylene glycol in the mixture of ethylene glycol and water, dimensionless
x	A spatial coordinate in a cartesian system, m
y	A spatial coordinate in a cartesian system, m
z	A spatial coordinate in a cartesian system; axial direction, m

Greek

β	Thermal expansion coefficient, 1/°C
γ	Electrical resistivity, Ω · m
δ	Distance from a node point to a control volume face at a given direction, m
Δ	Designates a difference
θ	Angular coordinate, °
μ	Dynamic viscosity, Pa · s
ρ	Density, kg/m^3

Subscripts

b	Bulk
cal	Calculated
E	Evaluated at neighboring node point to a given node point in eastern direction; refer to Fig. 23.1
e	Evaluated at eastern control volume interface of a given node point; refer to Fig. 23.1
e^+	Evaluated at eastern control volume interface of a given node point in side of neighboring node point; refer to Fig. 23.1
e^-	Evaluated at eastern control volume interface of a given node point in side of given node point; refer to Fig. 23.1
eg	Ethylene glycol
exp	Experimental
i	Index in radial direction
in	Evaluated at inlet
iw	Evaluated at inside wall of a tube
j	Index in circumferential direction
k	Index in axial direction
mix	Mixture of ethylene glycol and water
N	Evaluated at neighboring node point to a given node point in northern direction; refer to Fig. 23.1
n	Evaluated at northern control volume interface of a given node point; refer to Fig. 23.1
n^+	Evaluated at northern control volume interface of a given node point in side of neighboring node point; refer to Fig. 23.1
n^-	Evaluated at northern control volume interface of a given node point in side of given node point; refer to Fig. 23.1
out	Evaluated at outlet
ow	Evaluated at outside wall of a tube
P	Evaluated at a given node; refer to Fig. 23.1
S	Evaluated at neighboring node point to a given node point in southern direction; refer to Fig. 23.1
s	Evaluated at southern control volume interface of a given node point; refer to Fig. 23.1
s^+	Evaluated at southern control volume interface of a given node point in side of neighboring node point; refer to Fig. 23.1
s^-	Evaluated at southern control volume interface of a given node point in side of given node point; refer to Fig. 23.1
ss	Stainless steel

W	Evaluated at neighboring node point to a given node point in western direction; refer to Fig. 23.1
w	Evaluated at western control volume interface of a given node point (refer to Fig. 23.1); evaluated at inside wall of a tube
w^+	Evaluated at western control volume interface of a given node point in side of neighboring node point; refer to Fig. 23.1
w^-	Evaluated at western control volume interface of a given node point in side of given node point; refer to Fig. 23.1

Superscript

$-$	Average

References

Colburn, A. P. (1933), "A Method of Correlating Forced Convective Heat Transfer Data and a Comparison with Liquid Friction," *Trans. Am. Inst. Chem. Eng.*, vol. 29, pp. 174–210.

Davis J. R. (ed.) (1994), *Stainless Steels*, in series of ASM Specialty Handbook, ASM International, Materials Park, Ohio.

Farukhi M. N. (1973), *An Experimental Investigation of Forced Convective Boiling at High Qualities inside Tubes Preceded by 180 Degree Bend*, Ph.D. thesis, Oklahoma State University, Stillwater.

Ghajar, A. J. (2004), "Non-Boiling Heat Transfer in Gas-Liquid Flow in Pipes—a Tutorial," invited tutorial, *Proceedings of the 10th Brazilian Congress of Thermal Sciences and Engineering—ENCIT 2004*, Rio de Janeiro, Brazil, Nov. 29–Dec. 3.

Ghajar, A. J., Kim, J., Malhotra, K., and Trimble, S. A. (2004), "Systematic Heat Transfer Measurements for Air-Water Two-Phase Flow in a Horizontal and Slightly Upward Inclined Pipe," *Proceedings of the 10th Brazilian Congress of Thermal Sciences and Engineering—ENCIT 2004*, Rio de Janeiro, Brazil, Nov. 29–Dec. 3.

Ghajar, A. J., and Tam, T. M. (1994), "Heat Transfer Measurements and Correlations in the Transitional Region for a Circular Tube with Three Different Inlet Configurations," *Experimental Thermal and Fluid Science*, vol. 8, no. 1, pp. 79–90.

Ghajar, A. J., and Zurigat, Y. H. (1991), "Microcomputer-Assisted Heat Transfer Measurement/Analysis in a Circular Tube," *Int. J. Appl. Eng. Educ.*, vol. 7, no. 2, pp. 125–134.

Gnielinski, V. (1976), "New Equations for Heat and Mass Transfer in Turbulent Pipe and Channel Flow," *Int. Chem. Eng.*, vol. 16, no. 2, pp. 359–368.

Incropera, F. P., and DeWitt, D. P. (2002), *Introduction to Heat Transfer*, 4th ed., Wiley, New York.

Kays, W. M., and Crawford, M. E. (1993), *Convective Heat and Mass Transfer*, 3d ed., McGraw-Hill, New York.

Kim, D., and Ghajar, A. J. (2002), "Heat Transfer Measurements and Correlations for Air-Water Flow of Different Flow Patterns in a Horizontal Pipe," *Experimental Thermal and Fluid Science*, vol. 25, no. 8, pp. 659–676.

Linstrom, P. J., and Mallard, W. G. (eds.) (2003), *NIST Chemistry WebBook*, NIST Standard Reference Database no. 69, National Institute of Standards and Technology, http://webbook.nist.gov.

Patankar, S. V. (1991), *Computation of Conduction and Duct Flow Heat Transfer*, Innovative Research, Inc., Minn.

Sieder, E. N., and Tate, G. E. (1936), "Heat Transfer and Pressure Drop in Liquids in Tube," *Ind. Eng. Chem.*, vol. 29, pp. 1429–1435.